

## Evolution of stratification over the New England shelf during the Coastal Mixing and Optics study, August 1996–June 1997

Steve Lentz, Kipp Shearman, Steve Anderson, Al Plueddemann, and Jim Edson  
Woods Hole Oceanographic Institution, Woods Hole, Massachusetts, USA

Received 27 August 2001; revised 4 April 2002; accepted 13 June 2002; published 10 January 2003.

[1] To investigate the processes influencing the evolution of stratification over continental shelves a moored array was deployed on the New England shelf from August 1996 to June 1997. Temperature, salinity, and current observations spanning the water column were obtained at four midshelf sites, along with meteorological measurements at a central site to estimate the wind stress and the surface heat and freshwater fluxes. Four processes contributed to the seasonal evolution of the stratification. (1) The breakdown of the seasonal thermocline in fall was primarily due to wind forcing, not surface cooling, and occurred in four discrete steps associated with westward, along-coast wind stress events. Eastward wind stress events of similar magnitude did not reduce the stratification. (2) The water at midshelf remained stratified throughout most of the winter due to saltier shelf-slope front water displaced onshore by anomalously strong and persistent eastward alongcoast wind stresses. (3) The gradual redevelopment of the thermocline, beginning in April, was primarily a one-dimensional response to increasing surface heat flux. (4) Stratification in early April and throughout May was substantially enhanced by low-salinity water associated with river runoff from southern New England that was driven eastward and offshore by upwelling-favorable (eastward) wind stresses. *INDEX TERMS:* 4219 Oceanography: General: Continental shelf processes; 4227 Oceanography: General: Diurnal, seasonal, and annual cycles; 4536 Oceanography: Physical: Hydrography; 4223 Oceanography: General: Descriptive and regional oceanography; *KEYWORDS:* coastal oceanography, stratification, seasonal cycle, shelf-slope front, Middle Atlantic Bight

**Citation:** Lentz, S., K. Shearman, S. Anderson, A. Plueddemann, and J. Edson, Evolution of stratification over the New England shelf during the Coastal Mixing and Optics study, August 1996–June 1997, *J. Geophys. Res.*, 108(C1), 3008, doi:10.1029/2001JC001121, 2003.

### 1. Introduction

[2] To identify and understand processes influencing the evolution of stratification on continental shelves, a moored array was deployed on the New England shelf (Figure 1) from August 1996 to June 1997, as part of the Office of Naval Research's Coastal Mixing and Optics (CMO) program [Dickey and Williams, 2001]. Stratification influences a wide range of open ocean and continental shelf processes, such as vertical mixing, internal waves, surface and bottom boundary layer responses, and the wind-driven shelf circulation. Stratification over continental shelves can vary substantially on timescales from hours to seasons. Thus it is important to understand the processes that contribute to variations in stratification.

[3] The continental-shelf waters of New England undergo a large seasonal variation in stratification, primarily associated with a seasonal variation in water temperature [Bigelow, 1933; Mayer *et al.*, 1979; Beardsley *et al.*, 1985; Linder and Gawarkiewicz, 1998]. In summer, there is a strong thermocline at about 20 m depth (Figure 2a). Temperature differences across the thermocline are 8–10°C at midshelf.

Below the thermocline there is a band of cold water (<11°C) over the middle and outer shelf, commonly referred to as the “cold pool” [Houghton *et al.*, 1982]. Salinity over the shelf is about 32 (practical salinity scale) near the coast and increases with depth and distance offshore (Figure 2b). The thermal stratification breaks down during fall, presumably due to the increasing frequency of strong wind events and a transition from positive surface heat fluxes (warming the ocean) in summer to negative surface heat fluxes (cooling) in winter [Beardsley *et al.*, 1985]. As a result, most of the shelf is unstratified in winter (Figures 2c and 2d), with water temperatures typically 4–6°C and salinities about 33. Thermal stratification redevelops in spring as the frequency of winter storms decreases and the surface heat flux increases. While this qualitative picture has existed for some time, a detailed understanding of both the breakdown and development of the thermal stratification does not exist, in part because there have not been direct measurements of surface heat flux over the New England shelf. Thus, for example, the relative importance of wind-driven vertical mixing and surface cooling to the breakdown of the thermal stratification is not known. It is also unclear to what extent both the fall breakdown and spring development of stratification are essentially one-dimensional processes [e.g., Large *et al.*, 1994; Plueddemann *et al.*, 1995], or whether advective

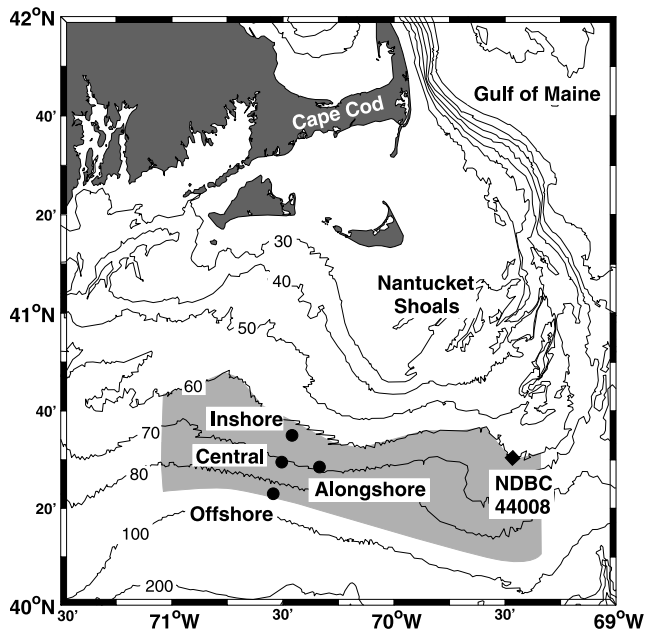


**Figure 1.** Map showing study area, mooring locations, and region covered by historical hydrographic observations (shaded region between 60-m and 90-m isobaths).

processes play an important role as found in coastal-upwelling regions [Lentz, 1987; Dever and Lentz, 1994].

[4] Stratification over the outer shelf off New England is also influenced by the presence of the shelf-slope front

which separates relatively fresh, cool shelf water from saltier, warmer slope water [Iselin, 1936] (Figure 2). Onshore excursions of the foot of the shelf-slope front enhance the near-bottom stratification over the outer shelf. The location of the foot of the shelf-slope front does not exhibit a large seasonal variation [Wright, 1976; Linder and Gawarkiewicz, 1998]. However, on shorter timescales, the foot of the front undergoes 10–20 km cross-isobath excursions in response to wind forcing [Boicourt and Hacker, 1976; Houghton et al., 1988].

[5] This study builds on results from previous field studies of the New England shelf, notably the Nantucket Shoals Flux Experiment (NSFE) [Beardsley et al., 1985] and the first Shelf Edge Exchange Program (SEEP-1) [Houghton et al., 1988]. Relative to these previous studies, the CMO measurements (described in section 2) include two new elements that are critical to understanding the evolution of the stratification. First, long-term (10 months), high-quality moored conductivity time series spanning the water column provide a direct assessment of the importance of salinity to the stratification and of the processes influencing the salinity variability. Second, a complete set of meteorological measurements over the New England shelf to estimate the various components of the atmospheric forcing, particularly the surface heat and freshwater fluxes. The primary objective of this study is to identify the dominant processes responsible for the observed evolution of the stratification over the 10-month CMO deployment and to assess the generality of those processes. The focus is on gross changes in the shelf stratification which tend to be associated with processes having timescales of days to

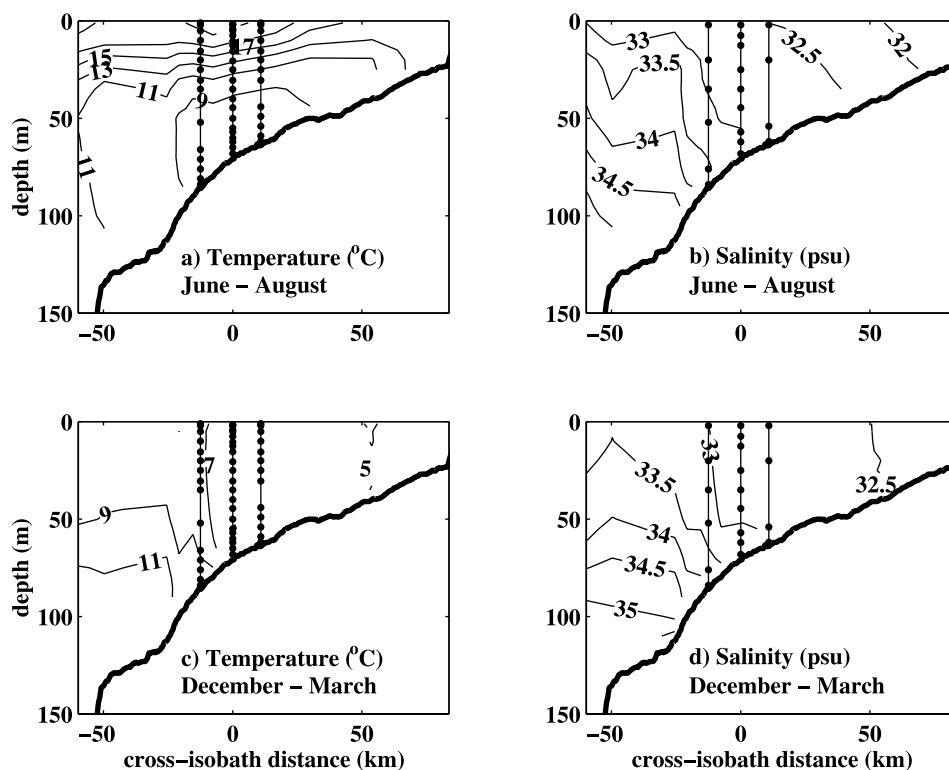


**Figure 2.** Mean cross-isobath sections of (left) temperature and (right) salinity for (a, b) summer and (c, d) winter. Moored temperature (left-hand panels) or conductivity (right-hand panels) sensor locations for the offshore, central, and inshore sites are also shown.

months. Thus, processes such as tidal currents, inertial motions, and internal waves, that may influence the stratification temporarily through advection or permanently through vertical mixing [MacKinnon and Gregg, 2001], are not examined. Based on an overview of the temperature and salinity variability in section 3, four features of the stratification variability are examined in detail in section 4: the fall breakdown of stratification, on/offshore movement of the foot of the shelf-slope front, intermittent salinity stratification in spring, and redevelopment of thermal stratification in spring.

## 2. Field Program and Data Processing

[6] The moored array consisted of four sites located on the outer half of the New England continental shelf south of Cape Cod, Massachusetts (Figure 1). The shelf south of New England is oriented roughly east-west and is about 100 km wide, with a bottom slope of 0.001. The moored array was deployed in a region with relatively straight isobaths (over scales of tens of kilometers) between more complex bathymetry onshore and the shelf break at about the 110-m isobath. The shelf offshore of the 40-m isobath narrows to the east because of Nantucket Shoals, which separates the New England shelf from the Gulf of Maine.

[7] The moored array consisted of a heavily instrumented central site on the 70-m isobath and three more lightly instrumented surrounding sites (Figure 1). The inshore site was 11 km onshore of the central site in 64 m of water, the offshore site was about 12.5 km offshore of the central site in 86 m of water, and the alongshore site was 14.5 km along-isobath toward the east from the central site. Temperature, conductivity, and current sensors spanning the water column were deployed on surface/subsurface mooring pairs at each site (Figure 2). (R. K. Shearman and S. J. Lentz, Mean and subtidal currents on the New England shelf during the Coastal Mixing and Optics Experiment, August 1996 to June 1997, manuscript in preparation for *Journal of Geophysical Research*, 2002, (hereinafter referred to as Shearman and Lentz, manuscript in preparation, 2002) will provide a detailed description of the subtidal current observations.) The central-site discus buoy also supported two complete sets of meteorological sensors, each of which measured wind speed and direction, air temperature, near-surface water temperature, relative humidity, incoming short and longwave radiation, atmospheric pressure, and precipitation. An acoustic anemometer and motion package also provided covariance estimates of wind stress. Ten-month time series were obtained from most of the instruments. There were gaps of 9 and 25 days during the fall in the near-surface observations from the inshore and alongshore sites, respectively, because the surface moorings broke free due to acoustic release failures.

[8] Processing of the data is described in detail by Galbraith *et al.* [1999]. Some of the conductivity time series exhibited offsets and drifts due to fouling of the conductivity cells. This problem was generally more severe near the bottom, suggesting the fouling was primarily due to suspended particles rather than biofouling. The offsets and drifts were identified and corrected (to the extent possible) by comparisons with adjacent instruments on the same mooring and shipboard CTD casts near the moorings.

Salinity and density were then estimated following Fofonoff and Millard [1983]. Measurement accuracies were approximately  $2 \text{ cm s}^{-1}$  for currents,  $0.05^\circ\text{C}$  for temperature, and 0.1 for salinity.

[9] Sampling intervals were 7.5 min or shorter for most of the instrumentation. Time series were low-pass filtered to remove variability having timescales shorter than an hour and decimated to hourly values to form a common time base. To focus on subtidal variability the hourly time series were low-pass filtered with a cutoff of 33 hours. Wind and current vectors were rotated into an along- and cross-isobath coordinate frame with  $x$  positive, eastward, toward  $110^\circ\text{T}$  and  $y$  positive onshore toward  $20^\circ\text{T}$ . Wind stress, surface heat flux, and evaporation were estimated from the meteorological measurements at the central site using the bulk formulas proposed by Fairall *et al.* [1996]. On the New England shelf, the subtidal along-isobath flow is most highly correlated with the component of the wind stress roughly aligned with the southern New England coastline [Beardsley *et al.*, 1985; Shearman and Lentz, manuscript in preparation, 2002]. This is qualitatively consistent with a geostrophic along-isobath flow generated by setup of a cross-shelf pressure gradient against the coastal boundary. An orientation of  $45^\circ\text{T}$  ( $65^\circ$  counterclockwise from the isobath orientation) was chosen to define along-coast wind stress  $\tau^{\text{scx}}$  (Shearman and Lentz, manuscript in preparation, 2002).

[10] To place the CMO observations in a broader temporal context, historical observations from the National Ocean Data Center (NODC) archive of shipboard temperature and salinity data were examined. The NODC archive includes 3625 temperature profiles and 503 salinity profiles in the region between  $71^\circ\text{W}$  and  $69.3^\circ\text{W}$  bounded by the 60-m and 90-m isobaths (Figure 1). These observations are uniformly distributed over this region and span the period from 1913 to 1996, though most of the temperature data were obtained between 1950 and the present and most of the salinity data were obtained between 1970 and the present. Wind observations from the Nantucket Lightship (1965–1982) and NDBC Buoy 44008 (1982–1999), both located 85 km east of the CMO central site, and discharge data for the Connecticut River (1928–1999) were also examined.

## 3. Overview of CMO Temperature and Salinity Variability

[11] In the following description “shelf water” will refer to salinities less than 32.5 and “shelf-slope front” water to salinities between 32.5 and 35.5, based on the observed temperature-salinity characteristics. The choice of 32.5 as the bounding salinity for shelf water is lower than in previous studies [Wright and Parker, 1976] because shelf salinities during the CMO deployment were lower than historical averages (see section 3.2). Shelf water was observed more than 95% of the time at the inshore site and more than 90% of the time in the upper 40 m at all four mooring sites. Shelf-slope front water was present about 80% of the time near the bottom at the offshore site.

[12] The subtidal temperature and salinity variability typically had spatial scales larger than the separation between the CMO moorings. Correlations between temper-



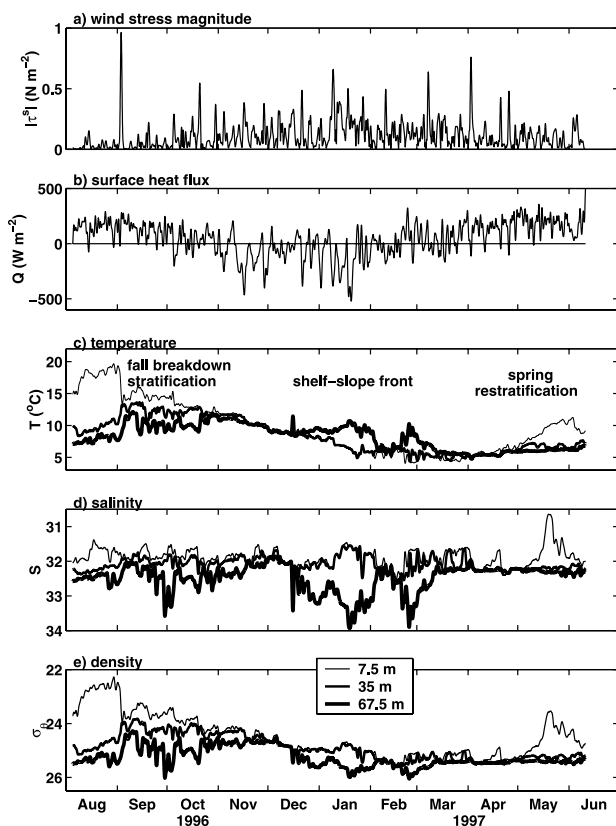


**Figure 3.** Subtidal time series of (a) wind stress magnitude, (b) net surface heat flux, (c) water temperature, (d) salinity, and (e) density from the central site during the CMO deployment. Near-surface, middepth, and near-bottom time series are shown for temperature, salinity, and density. The fall breakdown and spring development of stratification are evident. The water column is stratified in winter due to warmer and saltier shelf-slope front water near the bottom.

ature or salinity times series on different moorings were typically greater than 0.6. (Correlations greater than 0.4 are significantly different from zero at the 99% confidence level conservatively assuming an independence timescale of 10 days). Therefore we initially focus on the central site.

### 3.1. Temperature Variability

[13] The moored temperature time series exhibit a seasonal variation (Figures 3c, 4a, 4c, and 4e) that was similar at all four mooring sites and generally consistent with previous observations [Beardsley *et al.*, 1985]. In August, wind stresses were weak (Figure 3a), surface heat fluxes were positive (indicating warming of the ocean) (Figure 3b), and there was a strong thermocline over the shelf at about 10 m depth. Near-surface temperatures were 18–20°C, with cold-pool water (<11°C) below 20 m (Figures 3c and 4a). The thermal stratification decreased from September to November in response to storm events, becoming essentially unstratified ( $|\Delta T| < 0.1^\circ\text{C}$ ) in mid-November. There were strong wind stress events and negative surface heat fluxes (cooling) from November through January. However, beginning in mid-December near bottom temperatures increased while near-surface temperatures continued to

decrease, resulting in a substantial temperature inversion near the bottom that persisted for much of the winter (Figure 4c). The near-bottom temperature inversion was due to the onshore displacement of shelf-slope front water that was warmer and saltier than the overlying shelf water (Figures 4c and 4d). The near-surface to near-bottom temperature difference reached  $-7^\circ\text{C}$  (offshore site) in late January. Near-bottom temperatures decreased during March and the water column became well mixed again in early April. Wind stress magnitudes decreased and surface heating increased from March to June. As a result, near-surface temperatures began to rise in late March, and there was a steady increase in the temperature difference across the water column from mid-April through May (Figures 3c and 4e). Near-bottom temperatures remained fairly constant from mid-March to June, except at the outer-shelf site where warmer shelf-slope front was evident during May. Increasing surface temperatures and relatively constant near-bottom temperatures resulted in the development of thermal stratification and reestablishment of the cold pool.

[14] Monthly average along-coast wind stresses during the fall (August–December) were slightly more westward (downwelling favorable) in 1996 than in the historical data (Figure 5a). During winter and spring (January–May), monthly average along-coast wind stresses were anomalously eastward (upwelling favorable) in 1997 relative to the historical data, except for April. Near-surface and middepth temperatures at the central site in 1996–1997 were close to the historical monthly means except near the surface in September and October and at middepth in October (Figures 5b and 5c), when temperatures were less than the historical monthly means due, at least in part, to a hurricane (Edouard) in early September 1996 (Figure 3a). Near the bottom, water temperatures in 1996–1997 were below the historical monthly averages from October through December and above from January to March (Figure 5d).

### 3.2. Salinity Variability

[15] With the exception of the strong thermocline in August, temperature and salinity made similar contributions to the density variability (Figures 3c, 3d, and 3e). The largest salinity variability at the central site occurred near the bottom in fall and winter and near the surface in spring. The near-bottom salinity variability was associated with on/offshore displacements of the foot of the shelf-slope front (Figure 3d). While the foot of the front was intermittently present at the offshore site throughout the deployment, it was primarily evident at the inshore and central sites in winter and to a lesser extent in fall, but not in spring (Figures 4b, 4d, and 4f). Salinities in the upper water column generally ranged from 31.5 to 32.5 with the notable exception of an event in the last half of May with minimum salinities of 30.5 in the upper 20 m (Figure 3d) at all four sites.

[16] Salinities during CMO were generally 0.5–1 fresher than the historical monthly means (Figures 6b and 6c), except near the bottom during winter, when salinities were closer to the historical monthly averages because the foot of the shelf-slope front was farther onshore than normal (as indicated by the anomalously warm near-bottom temperatures in January–February, Figure 5d). Anomalously fresh water was also observed in the Gulf of Maine and on

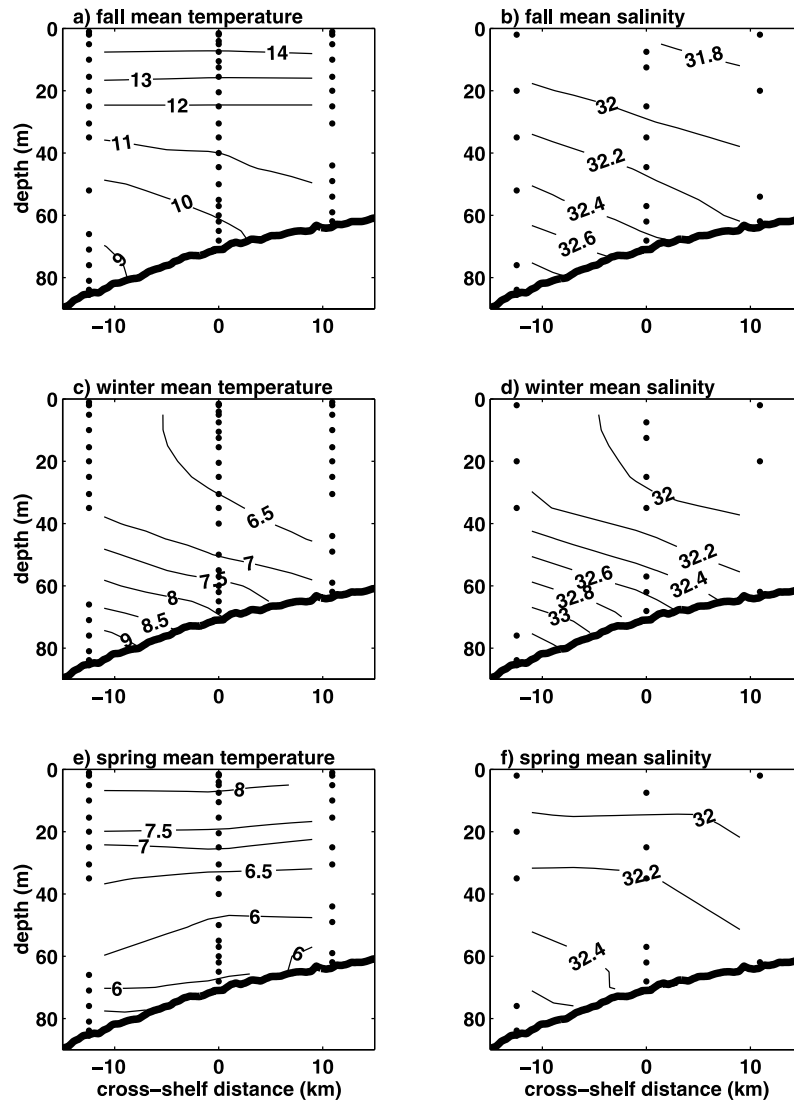


**Figure 4.** (left) Mean temperature and (right) salinity cross-isobath sections for (a, b) fall, (c, d) winter, and (e, f) spring from the moored array observations. Instrument locations are noted by dots.

Georges Bank beginning in early 1996 [Benway and Jossi, 1998; Smith *et al.*, 2001] indicating this was not a local phenomenon. Smith *et al.* [2001] suggest this anomalously fresh water had a northern source, possibly the Labrador Sea/Baffin Bay region. The anomalously fresh water during CMO is the reason for choosing a salinity of 32.5 as the dividing point between shelf and shelf-slope front water rather than a more traditional value around 33.5 [Wright, 1976]. This emphasizes one of the shortcomings of defining the shelf-slope front based on a particular isohaline or isotherm given large interannual variations in shelf water characteristics.

[17] Monthly variations in near-surface salinity during CMO are qualitatively consistent with the historical monthly means, salinities were roughly constant from August through April and lower in spring (May–July) (Figure 6b). The low salinities from May through July are presumably the result of freshwater transport from the Scotian shelf, and spring runoff from the Gulf of Maine or the southern New England shelf (Figure 6a) [Bigelow

and Sears, 1935; Ketchum and Corwin, 1964; Mountain and Manning, 1994]. The larger standard deviations in the historical near-surface salinities during summer and early fall relative to winter and spring are due to the prevalence of intrusions of shelf-slope front water. Near-bottom salinities at the central site during CMO were largest in winter and smaller during spring and fall, with the exception of an event in late September (Figure 6c). In contrast, historical monthly mean salinities near the bottom are largest in fall and smaller and relatively constant from winter through summer (January through August). The saltier near-bottom water in fall may be due to seasonal onshore migration of the foot of the shelf-slope front [Linder and Gawarkiewicz, 1998], seasonal variations in the alongslope transport, or seasonal variations in the salinity of the shelf-slope front water. Monthly mean salinities near the bottom include as few as 9–15 salinity profiles in October–December, and 40 profiles or less during the other months. (In contrast, there are 100 to over 350 temperature profiles in each monthly mean because of the large number of historical BT stations).

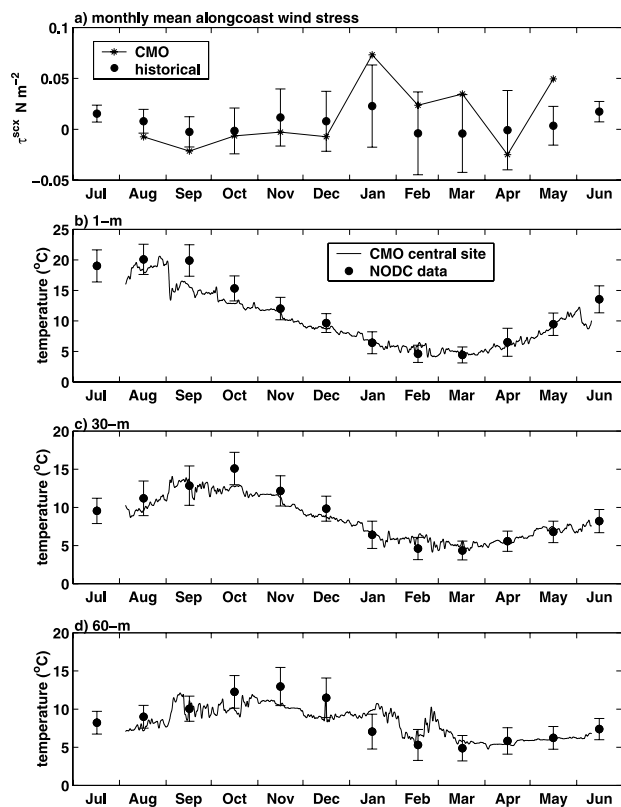


**Figure 5.** Comparison of (a) monthly mean alongcoast wind stress during CMO and from Nantucket Lightship/NDBC 44008 for the period from 1963–1999, and comparison of (b) near-surface, (c) middepth, and (d) near-bottom temperatures from the CMO central site with monthly means of the historical hydrographic data. Error bars denote  $\pm 1$  standard deviation.

Thus, while sensible patterns emerge from the monthly mean salinities, the results must be regarded with caution.

#### 4. Processes Influencing Stratification

[18] Based on the temperature and salinity variability described above, four features dominated subtidal variations in stratification during the CMO deployment: (1) the fall breakdown of stratification; (2) the movement of the foot of the shelf-slope front; (3) the near-surface, low-salinity events in May 1997; and (4) the spring development of thermal stratification. The processes that cause these variations in stratification are examined in the following sections.

##### 4.1. Fall Breakdown of Stratification

[19] The breakdown of stratification during the fall of 1996 occurred during four wind stress events, each lasting 1–2 days (peak, hourly wind stress magnitudes greater than  $0.4 \text{ N/m}^2$ , Figure 7 and Table 1). The resulting decrease in thermal stratification is consistent with vertical mixing as near-surface temperatures decreased and deeper temperatures increased during these events (Figure 3c). During the longer periods between these four events there was no systematic change in the thermal stratification (Figure 7a). The same step-like decrease in thermal stratification was

observed at all four sites, though it was less clear at the offshore site because of on/offshore movement of the foot of the shelf-slope front. (Temperature differences across the water column rather than salinity or density are shown in Figure 7a because salinity and density were more strongly influenced by movement of the foot of the shelf-slope front.)

[20] The most striking of the four events was Hurricane Edouard which passed about 100 km east of the moored array on September 2, as it tracked northeastward along the east coast of the United States. The other three events were two trailing cold fronts associated with low-pressure systems moving from west to east across the U.S on October 3 and October 18, and a high pressure system over the northeastern U.S. on November 14. During these four events maximum wind stress magnitudes were  $0.39$ – $1.21 \text{ N m}^{-2}$ , surface heat fluxes were  $215$  to  $-275 \text{ W m}^{-2}$ , and wave heights were  $3.3$  to  $7.3 \text{ m}$  (Table 1).

[21] A puzzling aspect of the observations is that four other fall events with maximum wind stress magnitudes greater than  $0.3 \text{ N m}^{-2}$  did not decrease the thermal stratification (Table 1, Figure 7). For example, wind stress events on October 29 and November 3 did not reduce the weak thermal stratification, even though there was also surface cooling during both events. There is not an obvious

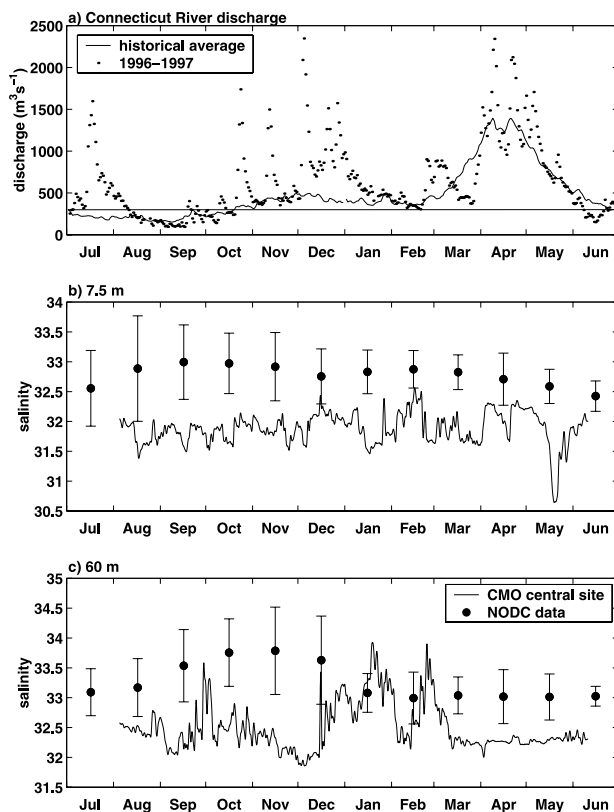


**Figure 6.** Time series of (a) average daily discharge from Connecticut River 1928–1999 (line) and the 1996 daily discharge (dots), and comparison of (b) near-surface and (c) near-bottom salinities from the CMO central site with monthly means of the historical hydrographic data. Error bars denote  $\pm 1$  standard deviation.

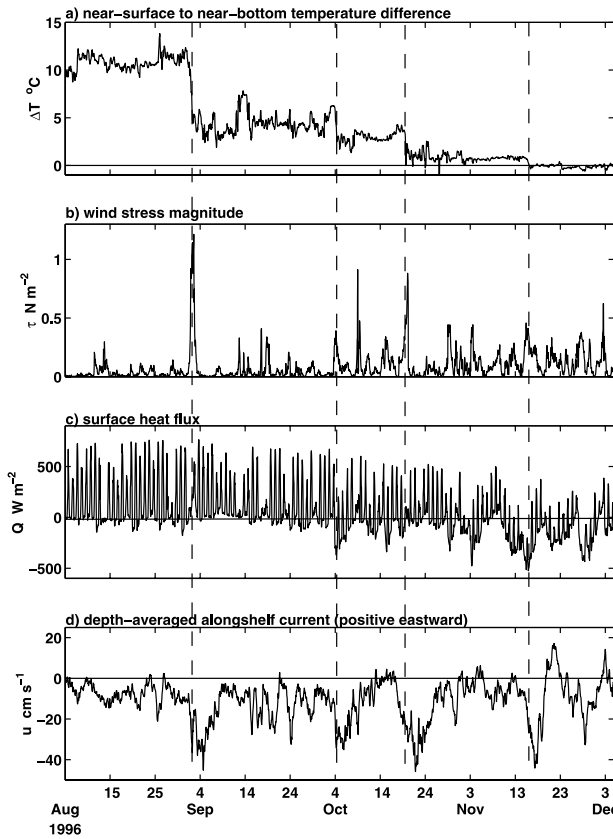


**Figure 7.** Time series from the central site of (a) the near-surface to near-bottom temperature difference, (b) wind stress magnitude, (c) surface heat flux, and (d) depth-averaged detided along-isobath current. Vertical dashed lines mark events that result in a lasting decrease in the thermal stratification.

relationship between reductions in thermal stratification and either surface cooling or surface wave height (Table 1). However, whether or not an event caused a reduction in thermal stratification does appear to depend on the direction of the alongcoast component of the wind stress  $\tau^{scx}$ . The four events that resulted in a reduction of the stratification had average alongcoast wind stresses that were westward with magnitudes of  $0.14 \text{ N m}^{-2}$  or more, while the other four events had weaker, eastward alongcoast wind stresses

(Table 1). Depth-averaged, along-isobath currents  $\langle u \rangle$  were strong ( $20\text{--}26 \text{ cm s}^{-1}$ ) and westward (negative) during the four events with strong westward alongcoast wind stresses and weaker (magnitudes less than  $12 \text{ cm s}^{-1}$ ) during the other four events. This is presumably because westward alongcoast wind stresses enhance the westward mean along-isobath flow on the New England shelf [Beardsley *et al.*, 1985; Shearman and Lentz, manuscript in preparation, 2002], while eastward wind stresses oppose the mean along-isobath flow. There were also larger near-surface to near-bottom shears in  $u$  during the four events that caused a reduction in the thermal stratification ( $\Delta u$ , Table 1). Cross-isobath currents near the bottom were offshore at  $5\text{--}9 \text{ cm s}^{-1}$  during the events that caused a reduction in stratification but were essentially zero ( $2$  to  $-2 \text{ cm s}^{-1}$ ) during the other four events. There was not an obvious pattern for either near-surface or depth-averaged cross-isobath currents. Westward alongcoast wind stresses also caused reductions in the vertical stratification in the spring of 1997 (section 4.4), while weaker eastward wind stresses did not.

[22] Why are westward (downwelling-favorable) wind stresses more effective than eastward (upwelling-favorable) wind stresses at reducing the stratification? One possibility is that the wind-forcing inhibits or enhances vertical mixing by increasing or decreasing the vertical stratification. On the New England shelf, and many other shelves, there is a cross-isobath density gradient because salinity increases with distance offshore due to river runoff (Figures 2b and 2d). Wind-driven cross-isobath advection acting on this cross-isobath density gradient may enhance or reduce the vertical stratification. For example, eastward alongcoast (upwelling-favorable) wind stresses would drive an offshore Ekman transport in the surface boundary layer that would tend to increase stratification by advecting lighter nearshore water offshore at the surface, while the opposing Ekman transport in the bottom boundary layer would carry denser offshore water onshore along the bottom. Westward (downwelling-favorable) wind stresses would have the opposite effect. While the wind-driven circulation at the CMO site is not this simple (Shearman and Lentz, manuscript in preparation, 2002), observations from CMO support the proposed relationship between wind stress and changes in stratification (top to bottom density differences  $\partial\Delta\sigma/\partial t$ ) (Figure 8). Eastward (positive) wind stresses typically increased the surface-to-bottom stratification, even though wind forcing should decrease near-surface stratifi-

**Table 1.** Various Parameters During the Four Wind Stress Events That Caused and Four Wind Stress Events That Did Not Cause a Reduction in the Stratification During the Fall of 1996<sup>a</sup>

Date	$\delta t$ , hours	$\delta\Delta T$ , $^{\circ}\text{C}$	$\delta\Delta\rho$ , $\text{kg m}^{-3}$	$ \tau_{max} $ , $\text{N m}^{-2}$	$\tau^{scx}$ , $\text{N m}^{-2}$	$\tau^{scy}$ , $\text{N m}^{-2}$	$Q$ , $\text{W m}^{-2}$	$H_{sig}$ , m	$\langle u \rangle$ , $\text{cm s}^{-1}$	$\Delta u$ , $\text{cm s}^{-1}$	$v^s$ , $\text{cm s}^{-1}$	$v^b$ , $\text{cm s}^{-1}$
Sep 1	31	5.86	1.52	1.21	-0.51	-0.45	215	7.3	-23	-24	-27	-7
Oct 3	33	4.36	1.28	0.39	-0.18	-0.12	-109	2.9	-25	-12	-14	-7
Oct 18	49	1.77	0.71	0.88	-0.25	0.21	-1	5.9	-20	-17	-1	-5
Nov 14	75	0.88	0.58	0.46	-0.19	-0.16	-275	3.3	-26	-8	-14	-9
Sep 18	19	0.27	-0.29	0.34	0.02	-0.22	54	3.1	-12	3	-30	1
Oct 14	42	-0.43	-0.12	0.34	0.08	-0.14	4	2.5	0	2	-14	-1
Oct 29	25	0.47	0.10	0.44	0.02	-0.31	-104	2.8	-5	1	-20	-2
Nov 3	31	0.20	-0.19	0.44	0.06	-0.23	-229	3.1	-2	1	-11	2

<sup>a</sup>See Figure 7. The duration of each event  $\delta t$  is defined as the length of time the wind stress magnitude was greater than  $0.1 \text{ N m}^{-2}$ . The  $\delta\Delta T$  and  $\delta\Delta\rho$  are changes in the top to bottom temperature and density difference during the event.  $|\tau_{max}|$  is the maximum wind-stress magnitude and  $H_{sig}$  is the wave height during each event. Other variables are averages over the duration of each event;  $\langle u \rangle$  is the depth-averaged along-isobath current and  $\Delta u$  is the top-to-bottom along-isobath current difference.



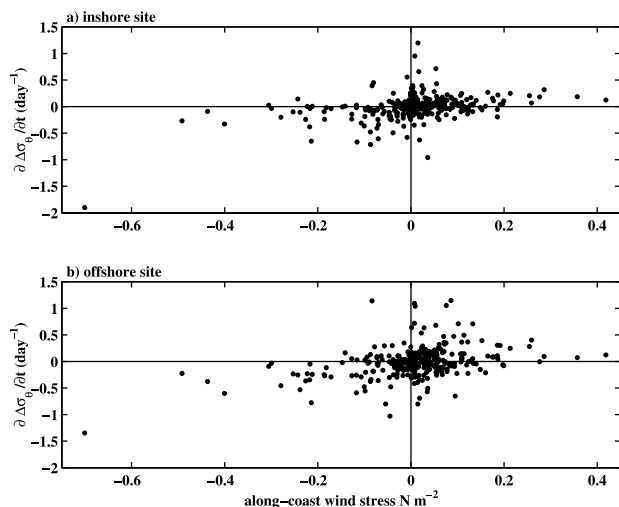


**Figure 8.** Daily values of the temporal change in depth-averaged stratification ( $\partial \Delta \sigma_\theta / \partial t$ ) at the (a) inshore and (b) offshore sites as a function of the along-coast wind stress  $\tau^{scx}$ . Note that for eastward (positive) wind stresses, the stratification ( $\Delta \sigma_\theta$ ) generally increases.

cation due to increased vertical mixing (see also Table 1). Westward wind stresses decreased the stratification.

[23] Another possibility is that wind forcing inhibits or enhances vertical mixing by decreasing or increasing the vertical shear in the horizontal currents. There was a mean thermal-wind shear associated with the cross-isobath density gradient during CMO such that the mean westward along-isobath flow decreased with depth (Shearman and Lentz, manuscript in preparation, 2002). Cross-isobath density differences between the inshore and offshore moorings indicate that this thermal-wind shear remained roughly the same during westward and eastward alongcoast wind stress events. Since the alongcoast wind stress is 65° counterclockwise from the local isobaths, the wind-driven shear, which tends to be to the right of the wind stress, has a large along-isobath component. Thus, during westward alongcoast wind stresses, the wind-driven shear would tend to enhance the mean thermal-wind shear (Table 1) increasing the likelihood of vertical mixing. During eastward alongcoast wind stresses, the wind-driven shear would tend to oppose the mean thermal-wind shear leading to a reduction in the total shear, decreasing the likelihood of vertical mixing. The relative importance of these two mechanisms, wind-driven advection changing the vertical stratification or the vertical shear, is the subject of ongoing research that includes a more detailed examination of the observations and numerical modeling.

[24] Previous studies [Mayer *et al.*, 1979; Beardsley *et al.*, 1985] and the historical hydrographic observations (Figure 5) indicate that the breakdown of stratification usually occurs between September and November over the New England shelf. It is unclear whether the fall breakdown of stratification is typically due to strong westward along-coast wind stresses as observed during CMO. Strong westward alongcoast wind stresses (magnitudes greater than 0.2 N m<sup>-2</sup>) during the fall were only slightly more common in 1996 (5% of the time) than in the historical wind observations (3% of the time). The

previous 1979 NSFE observations are ambiguous because the shallowest temperature measurements at midshelf were at about 30 m depth in late fall [Beardsley *et al.*, 1985] and the presence of the shelf-slope front complicates interpretation of the SEEP-1 observations [Houghton *et al.*, 1988].

#### 4.2. Onshore/Offshore Movement of the Shelf-Slope Front

[25] The presence or absence of the foot of the shelf-slope front dominated variability in the stratification in the lower half of the water column over the outer shelf during the entire CMO deployment (Figure 9c). Shelf-slope front water (salinities greater than 32.5 and warmer water near the bottom) extended farthest onshore during periods of strong and persistent eastward, alongcoast wind stresses (upwelling favorable) in mid-December through January and mid-February through early March (Figure 9). This suggests some of the variability in the location of the foot of the shelf-slope front, and hence in near-bottom temperature and salinity, may have been driven by the wind stress.

[26] Previous studies over the New England shelf suggest wind-driven movement of the foot of the shelf-slope front is fairly common, particularly in winter. Near-bottom temperature inversions from December 1979 through March 1980 at the NSFE N3 mooring indicate the foot of the shelf-slope front extended onshore of the 88-m isobath during eastward alongcoast wind stresses but not during westward along-

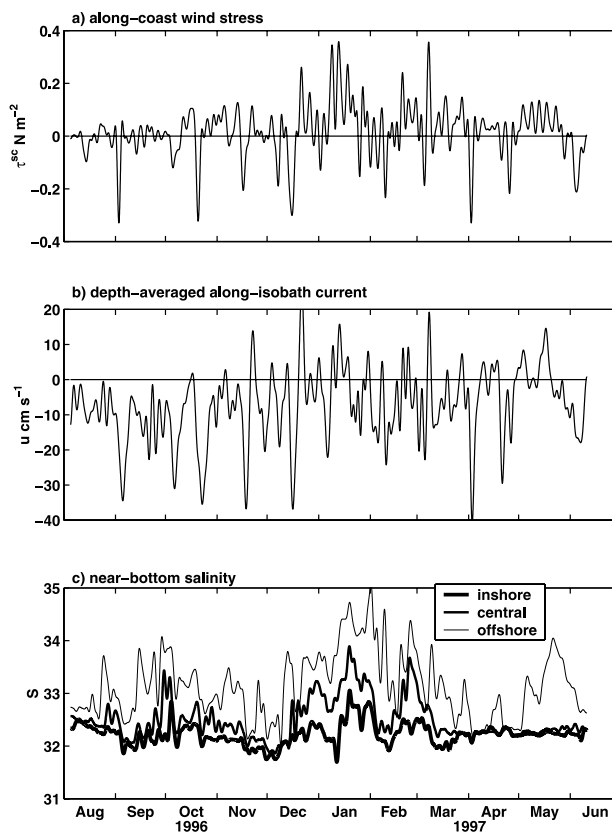


**Figure 9.** Low-pass filtered time series of (a) along-coast wind stress, (b) depth-averaged along-isobath current at the central site, and (c) near-bottom salinities at the inshore, central, and offshore sites.



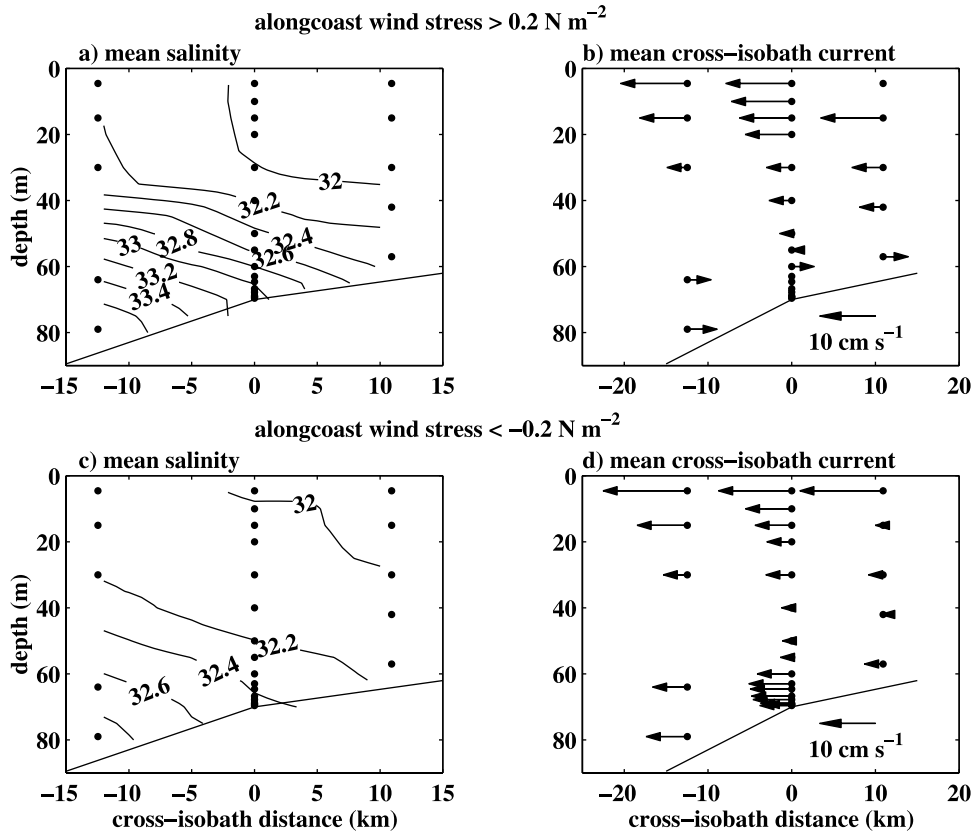


**Figure 10.** Cross-sections of (a) mean salinity and (b) mean cross-isobath velocity profiles for all times when alongcoast wind stresses were greater than  $0.2 \text{ N m}^{-2}$ , that is, strong upwelling favorable wind stresses, and (c) mean salinity and (d) mean cross-isobath velocity profiles for all times when alongcoast wind stresses were less than  $-0.2 \text{ N m}^{-2}$ , that is, strong downwelling favorable wind stresses. Conductivity and current sensor locations are indicated by dots. Data are from the inshore, central, and offshore moorings and from a bottom tripod at the central site.

coast wind stresses [Beardsley *et al.*, 1985]. In SEEP-1, Houghton *et al.* [1988] noted that movement of the foot of the shelf-slope front over timescales from 2 to 10 days was correlated with the alongcoast wind stress during the winter of 1983–1984 and that the relationship was qualitatively consistent with a simple model proposed by Boicourt and Hacker [1976]. The alongcoast wind stress drives an along-isobath current throughout the water column and the resulting bottom stress forces a cross-isobath Ekman transport that displaces the foot of the front on or offshore. The CMO observations are also qualitatively consistent with this model (Figure 10). During strong eastward (positive) wind stresses, the typically westward along-isobath flow reverses to eastward (Figure 9b) and there is an onshore flow near the bottom (Figure 10b) that displaces the foot of the shelf-slope front onshore (Figure 10a), thus increasing the near-bottom salinity. Westward wind stresses have the opposite effect (Figures 10c and 10d). (The persistent offshore flow in the upper 30 m includes both a geostrophic component and an Ekman component due to the along-isobath, rather than alongcoast, wind stress (Shearman and Lentz, manuscript in preparation, 2002)).

[27] The conceptual model proposed by Boicourt and Hacker [1976] includes three basic assumptions. First,

near-bottom salinity variations are due to cross-isobath advection, which from the time-integrated salt balance is

$$S^b(t) - S^b(t=0) \approx - \int_0^t v^b S_y^b dt, \quad (1)$$

where  $S^b$  and  $v^b$  are the near-bottom salinity and cross-isobath current, and  $S_y^b$  is the near-bottom cross-isobath salinity gradient associated with the shelf-slope front. Second, near-bottom cross-isobath velocities are related to the along-isobath bottom stress through an Ekman balance, and third, the bottom stress is proportional to the wind stress, i.e.,

$$v_b \approx \frac{\tau^{bx}}{\rho_o f \delta^b} \sim \frac{a \tau^{sxc}}{\rho_o f \delta^b}, \quad (2)$$

where  $\rho = 1025 \text{ kg m}^{-3}$ ,  $f = 0.94 \times 10^{-4} \text{ s}^{-1}$ ,  $\delta^b$  is the boundary layer height, and  $a$  is a proportionality constant relating the alongcoast wind stress to the along-isobath bottom stress.

[28] To our knowledge there has not been a quantitative test of this model to determine how much of the near-

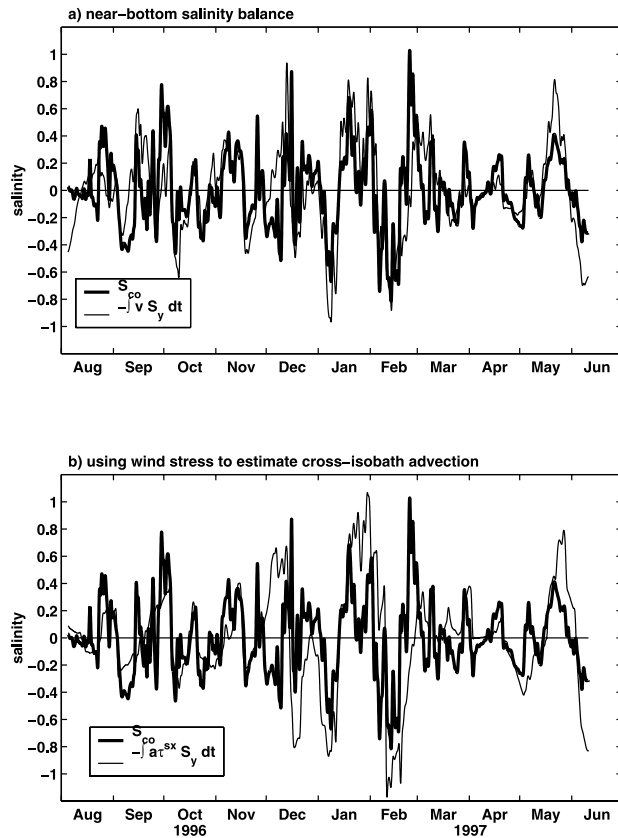


**Figure 11.** (a) Comparison of the terms in equation (1), the average of central and offshore site near-bottom salinities  $S_{co}$  and the cumulative cross-isobath salt flux. (b) Comparison of  $S_{co}$  and an estimate of the cumulative cross-isobath salt flux using equation (2) and the along-coast wind stress to estimate the near-bottom cross-isobath velocity.

bottom salinity variability is wind forced. Therefore, the CMO observations are used to test this simple model and the underlying assumptions. The assumption that near-bottom salinity variations are due to cross-isobath advection is examined first. The cross-isobath salt flux, the right-hand-side of equation (1), is estimated using the average of the near-bottom cross-isobath velocities at the central and offshore sites and the near-bottom salinity difference between the central and offshore sites to estimate  $S_y^b$ . (Near-bottom cross-isobath currents at these two moorings are significantly correlated, suggesting the moorings are close enough together to provide reasonable estimates of the cross-isobath salt flux.) Cross-isobath advection accounts for most of the major features in the salinity time series having timescales from a few days to a month (Figure 11a). The correlation is 0.64, which is significant at the 99% confidence level. There is similar agreement between estimates of the terms in equation (1) using the central and inshore sites (correlation 0.53), and for the two terms in the corresponding near-bottom heat balance (correlations 0.64 inshore-central and 0.62 central-offshore). The time series in Figure 11 have been band-pass filtered to retain timescales from 1.5 days to 60 days. There is poor agreement between the two time series at longer timescales, possibly because small errors in

the low-frequency current, or the current orientation relative to the salinity gradient estimate, result in large errors in the time integrated flux. It is also possible that at longer timescales, other terms, such as vertical mixing, dominate the salt and heat balances.

[29] Covariance estimates of along-isobath bottom stress from bottom tripod measurements at the central site [Shaw *et al.*, 2001] are correlated with the alongcoast wind stress. The maximum correlation is 0.66 for bottom stress lagging the alongcoast wind stress by 15 hours. This is consistent with previous studies that have shown a correlation between the alongcoast wind stress and the along-isobath flow at subtidal timescales [Beardsley *et al.*, 1985; Shearman and Lentz, manuscript in preparation, 2002]. However, the magnitude of the bottom stress is only about 10% of the wind stress, so bottom stress does not balance the wind stress at this site (Shearman and Lentz, manuscript in preparation, 2002). Near-bottom cross-isobath currents are correlated with the along-isobath bottom stress (correlations  $\sim 0.6$ ), consistent with a bottom Ekman layer response (Figures 10b and 10d), and are also correlated with the alongcoast wind stress (correlations 0.4–0.5). Correlations between cross-isobath currents and either the alongcoast wind stress or the along-isobath bottom stress were only significant within about 10 m of the bottom. At the central site, where there were seven current meters within 10 m of the bottom, the correlations and regression coefficients between  $v$  and  $\tau^{scx}$  or  $\tau^{bx}$  were vertically uniform within 10 m of the bottom. From equation (2) the regression coefficient between  $v^b$  and  $\tau^{bx}$  should be approximately  $1/(\rho_o f \delta^b) \approx 1.0 \text{ m s}^{-1} / \text{N m}^{-2}$ , assuming  $\delta^b \approx 10 \text{ m}$ . The regression coefficient estimated from the observations was about one third of this value. The reason for the discrepancy is not clear.

[30] Estimates of the time-integrated salt flux, using along-coast wind stress and equation (2) to estimate  $v_b$  with  $a = 0.25$ , are significantly correlated (99% confidence level) with near-bottom salinity variability (Figure 11b), though the correlation is not large (0.48). (The choice of  $a = 0.25$  crudely accounts for both the relationship between the wind stress and bottom stress and the relationship between the bottom stress and the near-bottom velocity.) Interestingly, using the along-isobath bottom stress rather than wind stress does not significantly improve the correlation (0.49). A number of factors probably contribute to discrepancies between the wind-driven estimates and the observed salinity variability. Discrepancies in early December and late February may be associated with along-isobath advection of salt (Figure 11a). The crude estimates of the cross-isobath salinity gradient and variability in the relationship between surface stress and near-bottom velocity probably also contribute to a decrease in the correlation. Nevertheless, these observations indicate that wind forcing is a substantial factor driving variability in the location of the foot of the shelf-slope front, and hence in the near-bottom temperature and salinity over the middle to outer shelf, throughout the CMO deployment.

[31] Wind forcing of the shelf-slope front also accounts, at least in part, for differences between the historical monthly means and the CMO near-bottom temperatures and salinities (Figures 5d and 6c). In January–March when near-bottom temperatures and salinities were larger than the

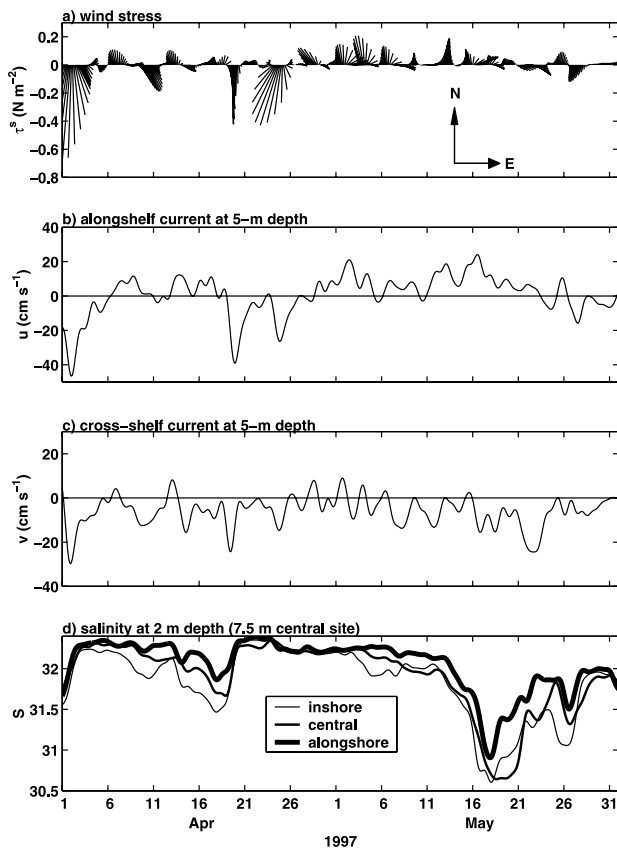


**Figure 12.** Low-pass filtered time series of (a) wind stress vectors (north toward top of figure), (b) along-isobath near-surface current, (c) cross-isobath near-surface current, and (d) near-surface salinities at the inshore, central, and alongshore sites.

historical monthly means, monthly mean wind stresses were more eastward than normal (Figure 5a). During October–December 1996, when near-bottom temperatures were lower than normal, monthly mean wind stresses were slightly more westward than normal.

### 4.3. Spring Salinity Stratification

[32] Freshening and warming of the near-surface waters both contributed to redevelopment of stratification in the spring of 1997. Temperatures increased steadily in response to surface heating, while salinity changes were more intermittent (Figures 3c and 3d). The processes accounting for the salinity stratification and the redevelopment of the season thermocline are examined below and in section 4.4, respectively.

[33] There were two events, one in mid-April and the other during most of May, when relatively fresh (salinities less than 32) water was observed in the upper 20–30 m of the water column at all four mooring sites (Figure 12d) resulting in a substantial increase in stratification (Figure 3e). The May event was fresher (minimum salinities  $\approx 30.5$ ) and persisted for longer (20–25 days) than the April event (10 days).

[34] One possible source for the relatively fresh water is the Gulf of Maine or the Scotian shelf, since the mean flow on the New England shelf is westward and buoyant water

tends to propagate with the coast to the right in the northern hemisphere. However, several factors indicate that this relatively fresh water came from the northwest rather than the east. The near-surface water tends to be freshest at the inshore site and saltiest at the alongshore site during both events (Figure 12d). Near-surface salinity maps from ship-board SeaSoar surveys in May also show the freshest water to the northwest [O'Malley *et al.*, 1998]. The near-surface currents during both the April and May events were eastward and offshore due to moderate northeastward wind stresses (Figures 12 and 13), consistent with the fresher water arriving first at the inshore site, then at the central site, and finally at the alongshore and offshore sites (Figure 12d). Arrival at the alongshore site lagged arrival at the central site by about a day indicating eastward along-isobath advection of about  $0.15 m s^{-1}$ , consistent with observed currents (Figure 12b). Reversals to westward along-isobath flow due to westward wind stress events (April 19 and May 28) resulted in the abrupt disappearance of the fresher water from the mooring sites, again indicating the low-salinity water came from the west rather than the east. The abrupt disappearance of the low-salinity water appears to be due to advection rather than vertical mixing since there was not a corresponding decrease in the deeper salinities.

[35] These results suggest the likely source of the fresh-water was runoff from southern New England, notably the Connecticut River (Figure 6a). Surface salinity maps from quarterly hydrographic surveys of the Northeastern U.S.

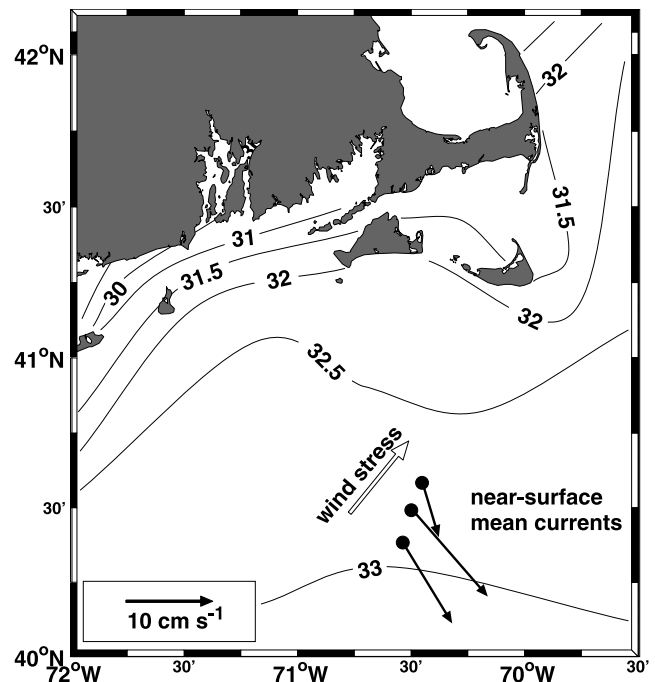


**Figure 13.** Map of the mean near-surface salinity for spring (March–May) over the New England shelf from historical hydrographic data. The mean wind stress at the central site and near-surface (4.5–15 m depth) currents at the inshore, central, and offshore sites for 12–21 May 1997 (low-salinity event in Figure 12d) are also shown. The mean wind stress magnitude is  $0.07 N m^{-2}$ . The mean flow swept low-salinity water from the northwest to the CMO site.

shelf taken as part of the Marine Resources Monitoring, Assessment, and Prediction (MARMAP) program [Manning and Holzwarth, 1990] and the mean surface salinity for March through May from the historical hydrographic data (Figure 13) show a region of low-salinity water in Long Island sound extending to the eastern end of Long Island associated with the peak discharge of the Connecticut River in spring [Ketchum and Corwin, 1964; Garvine, 1974] (Figure 6a). A discharge of  $1000 \text{ m}^3/\text{s}$  during April (Figure 6a) would result in an approximately  $10,000 \text{ km}^2$  pool of water 10 m thick with a salinity anomaly of 1 indicating the Connecticut River discharge was sufficient to account for the observed low-salinities at the CMO sites in April and May. In summary, northeastward winds forced southeastward near-surface flows that brought low-salinity water from the southern New England coastal region to the CMO site in mid-April and May 1997 (Figure 13).

[36] Salinities of less than 31.5 in this region, as observed in May 1997, are rare. Near-surface salinities less than 31.5 were only observed in 3 of 77 observations during spring (March–June) in the region between the 60- and 90-m isobaths and between  $71^\circ\text{W}$  and  $70.5^\circ\text{W}$ . Two of the observations were on June 1, 1978 and the third was on April 6, 1996. There were moderate eastward wind stresses prior to both these events. Near-surface salinities less than 31.5 in spring were not found in 323 profiles from the region farther east, between the 60- and 90-m isobaths extending from  $70.5^\circ\text{W}$  to  $69^\circ\text{W}$ . The Connecticut River discharge in the spring of 1997 was fairly typical (Figure 6a). However, monthly-mean alongcoast wind stresses were anomalously eastward in May 1997 relative to the historical monthly mean (Figure 5a). This suggests the anomalously fresh water at the CMO site in May was due to the unusually persistent eastward winds in May, not anomalously large runoff. Whether less extreme events such as the one in April 1997 are common is less clear. Eastward alongcoast wind stresses greater than  $0.1 \text{ N m}^{-2}$  occur about 15% of the time in March, 10% of the time in April and 5% or less of the time from May through August, indicating the likelihood of low-salinity coming from the northwest decreases through the spring. This combined with the low average discharge from the Connecticut River after May (Figure 6a) suggests the lower-salinity water in June and July evident in the monthly means from the historical hydrographic data (Figure 6b) is probably advected westward from the Gulf of Maine and Scotian shelf [Bigelow and Sears, 1935].

#### 4.4. Spring Development of the Seasonal Thermocline

[37] The development of thermal stratification during CMO began after a storm on April 1 that temporarily resulted in a well-mixed water column at the central site (Figure 14). Prior to this storm, near-bottom waters were warmer than near-surface waters, suggesting shelf-slope front water was present at the central site. After the April 1 storm there was a steady increase in near-surface temperatures and thermal stratification through early June. The historical hydrographic observations indicate that the increases in both temperature and thermal stratification during CMO were typical (Figures 5b–5d). The warming of the water column in spring 1997 was primarily due to surface heating. Assuming advection was not important and

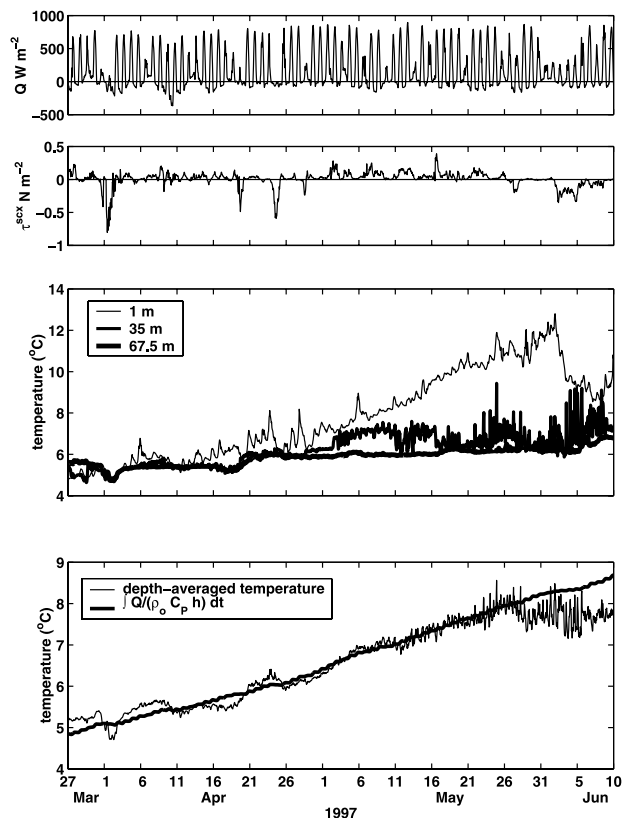


**Figure 14.** Time series of the (a) surface heat flux, (b) along-coast wind stress, (c) central site water temperature, and (d) comparison of the depth-averaged temperature and the cumulative surface temperature flux. The temperature flux has been shifted to facilitate comparison.

integrating the depth-averaged, one-dimensional heat balance forward in time yields

$$T(t) = T(t=0) + \int_0^t \frac{Q}{\rho_o C_P h} dt, \quad (3)$$

where  $\rho_o$  is average density,  $C_P = 4 \times 10^6 \text{ W s } ^\circ\text{C}^{-1} \text{ m}^{-3}$  is the heat capacity of sea water,  $h = 70 \text{ m}$  is the water depth,  $T$  is the depth-averaged temperature,  $t$  is time, and  $Q$  is the net surface heat flux. The cumulative surface heat flux accounts for most of the observed increase in the depth-averaged temperature (Figure 14d) from late March through May.

[38] The general tendency for westward alongcoast wind stresses to reduce the thermal stratification and for eastward wind stresses to be ineffective in reducing the thermal stratification in fall (section 4.1) was also observed in spring. Three westward (negative) along-coast wind stress events in late April resulted in temporary reductions of the thermal stratification, but a subsequent sequence of moderate ( $>0.1 \text{ N m}^{-2}$ ) eastward (positive) wind stress events in May had little impact on the thermal stratification. As discussed in the previous section, this period of eastward wind stress resulted in a substantial increase in the near-surface salinity stratification (Figure 12) that presumably inhibited vertical mixing consistent with the results for fall. There was a substantial reduction in thermal stratification in early June associated with a prolonged westward wind



stress event. The reduction in stratification appears to have been primarily due to vertical mixing, though the differences between the depth-averaged temperature and the cumulative heat flux (Figure 14d) indicates advection was also important during the June event.

[39] These results indicate that while the spring development of thermal stratification was primarily a gradual, one-dimensional response to surface heating, westward (downwelling-favorable) wind stress events in spring can have a substantial impact on the seasonal evolution of the temperature and thermal stratification. Vertical mixing associated with westward wind stress events decreased the near-surface temperatures and increased the deep, cold-pool temperatures (April 20 and early June events) resulting in reduced thermal stratification. The reduced thermal stratification makes the shelf waters more susceptible to vertical mixing from subsequent wind events. This suggests that the direction, magnitude, and timing of spring wind-stress events may play an important role in interannual variations in summer water temperatures and stratification.

## 5. Summary

[40] The processes causing subtidal variations in stratification over the New England shelf between August 1996 and June 1997 were investigated using moored observations obtained during the Coastal Mixing and Optics study. Four features dominated the observed changes in stratification. The wind forced, cross-isobath circulation acting on the cross-isobath salinity gradients played an important role in each of these processes.

- The destruction of the seasonal thermocline in fall 1996 occurred during four events associated with westward alongcoast wind stresses. Eastward along-coast wind stresses of similar magnitude did not reduce the thermal stratification and surface cooling was not a substantial factor in the breakdown of the thermal stratification.

- Variability in stratification in the lower half of the water column on the outer shelf was due, in part, to wind-forced, on-offshore movement of the foot of the shelf-slope front. During the winter of 1996–1997, the foot of the shelf-slope front extended onshore to midshelf and near-bottom waters remained warm and stratified throughout the winter, as a result of anomalously strong and persistent eastward wind stresses.

- Redevelopment of thermal stratification was primarily a gradual, one-dimensional process driven by the seasonal increase in surface heat flux. However, the timing and magnitude of westward wind stress events in spring influenced the development of the thermocline by mixing the heat that accumulated near the surface down into the lower water column.

- In April and May of 1997, low-salinity water associated with runoff from the Connecticut River, was carried eastward and offshore to midshelf by persistent northeastward wind stresses. The contribution of this 20 m thick layer of low salinity water to the spring stratification was as substantial as the developing seasonal thermocline.

[41] **Acknowledgments.** The design, deployment, and recovery of the moored array, the preparation of the instruments, and processing of the data were done by N. Galbraith, W. Ostrom, R. Payne, R. Trask, G. Tupper,

J. Ware, and B. Way of the Upper Ocean Processes Group with assistance from M. Baumgartner, C. Marquette, Lt. M. Martin, N. McPhee, E. Terray, and S. Worriow. The moorings were fabricated by the WHOI Rigging Shop under the direction of D. Simoneau. The success of the field program was a direct result of the exceptional efforts of all those involved and that effort is greatly appreciated. Thoughtful comments on the manuscript by Glen Gawarkiewicz are greatly appreciated. Suggestions by two anonymous reviewers also improved the manuscript. The work was funded by the Office of Naval Research, Code 322, under grant N00014-95-1-0339.

## References

- Beardsley, R. C., D. C. Chapman, K. H. Brink, S. R. Ramp, and R. Schlitz, The Nantucket Shoals Flux Experiment (NSFE79), I, A basic description of the current and temperature variability, *J. Phys. Oceanogr.*, 15, 713–748, 1985.
- Benway, R. L., and J. W. Jossi, Departures of 1996 temperatures and salinities in the Middle Atlantic Bight and Gulf of Maine from historical means, *J. Northwest. Atl. Fish. Sci.*, 24, 61–86, 1998.
- Bigelow, H. B., Studies of the waters on the continental shelf, Cape Cod to Chesapeake Bay, I, The cycle of temperature, *Pap. Phys. Oceanogr. Meteorol.*, 2, 1–135, 1933.
- Bigelow, H. B., and M. Sears, Studies of the waters on the continental shelf, Cape Cod to Chesapeake Bay, II, Salinity, *Pap. Phys. Oceanogr. Meteorol.*, 4, 1–94, 1935.
- Boicourt, W. C., and P. W. Hacker, Circulation on the Atlantic continental shelf of the United States, Cape May to Cape Hatteras, in *Memoires de la Societe Royale des Sciences de Liege*, edited by J. C. J. Nihoul, pp. 187–200, Univ. of Liege, Liege, Belgium, 1976.
- Dever, E. P., and S. J. Lentz, Heat and salt balances over the northern California shelf in winter and spring, *J. Geophys. Res.*, 99, 16,001–16,017, 1994.
- Dickey, T. D., and A. J. Williams III, Interdisciplinary ocean process studies on the New England shelf, *J. Geophys. Res.*, 106, 9427–9434, 2001.
- Fairall, C. W., E. F. Bradley, D. P. Rogers, J. B. Edson, and G. S. Young, Bulk parameterization of air-sea fluxes for Tropical Ocean-Global Atmosphere Coupled-Ocean Atmosphere Response Experiment, *J. Geophys. Res.*, 101, 3747–3764, 1996.
- Fofonoff, N. P., and R. C. Millard Jr., Algorithms for computation of fundamental properties of seawater, *UNESCO Tech. Pap. Mar. Sci.*, 44, 53 pp., 1983.
- Galbraith, N., A. Plueddemann, S. Lentz, S. Anderson, M. Baumgartner, and J. Edson, Coastal Mixing and Optics Experiment moored array data report, *Tech. Rep. WHOI-99-15*, 156 pp., Woods Hole Oceanogr. Inst., Woods Hole, Mass., 1999.
- Garvine, R. W., Physical features of the Connecticut River outflow during high discharge, *J. Geophys. Res.*, 79, 831–846, 1974.
- Houghton, R. W., R. Schlitz, R. C. Beardsley, B. Butman, and J. L. Chamberlain, The Middle Atlantic Bight cold pool: Evolution of the temperature structure during summer, 1979, *J. Phys. Oceanogr.*, 12, 1019–1029, 1982.
- Houghton, R. W., F. Aikman III, and H. W. Ou, Shelf-slope frontal structure and cross-shelf exchange at the New England shelf-break, *Cont. Shelf Res.*, 8, 687–710, 1988.
- Iselin, C. O., A study of the circulation of the western North Atlantic, *Pap. Phys. Oceanogr. Meteorol.*, 4, 1–101, 1936.
- Ketchum, B. H., and N. Corwin, The persistence of “winter” water on the continental shelf south of Long Island, New York, *Limnol. Oceanogr.*, 9, 467–475, 1964.
- Large, W. G., J. C. McWilliams, and S. C. Doney, Oceanic vertical mixing: A review and a model with a nonlocal boundary layer parameterization, *Rev. Geophys.*, 32, 363–403, 1994.
- Lentz, S. J., A heat budget for the northern California shelf during CODE 2, *J. Geophys. Res.*, 92, 14,491–14,509, 1987.
- Linder, C. A., and G. Gawarkiewicz, A climatology of the shelfbreak front in the Middle Atlantic Bight, *J. Geophys. Res.*, 103, 18,405–18,423, 1998.
- MacKinnon, J. A., and M. C. Gregg, Mixing on the late-summer New England shelf: Solibores and stratification, *J. Phys. Oceanogr.*, submitted, 0–0, 2001.
- Manning, J., and T. Holzwarth, Description of oceanographic conditions on the Northeast continental shelf: 1977–1985, *Tech. Rep. Northeast Fish. Cent. Ref. Doc. 90-04*, 373 pp., NOAA/National Marine Fish. Serv., Northeast Fish. Cent., Woods Hole, Mass., 1990.
- Mayer, D. A., D. V. Hansen, and D. A. Ortman, Long-term current and temperature observation on the Middle Atlantic shelf, *J. Geophys. Res.*, 84, 1776–1792, 1979.
- Mountain, D. G., and J. P. Manning, Seasonal and interannual variability in the properties of the surface waters of the Gulf of Maine, *Cont. Shelf Res.*, 14, 1555–1581, 1994.

- O'Malley, R., J. A. Barth, A. Erofeev, J. Fleischbein, P. M. Kosro, and S. D. Pierce, SeaSoar CTD observations during the Coastal Mixing and Optics Experiment: R/V Endeavor Cruises from 14-Aug to 1-Sep 1996 and 25-Apr to 15-May 1997, *Tech. Rep. 98-1*, 499 pp., Coll. of Oceanic and Atmos. Sci., Oreg. State Univ., Corvallis, Oreg., 1998.
- Plueddemann, A. J., R. A. Weller, M. Stramska, T. Dickey, and J. Marra, Vertical structure of the upper ocean during the Marine Light-Mixed Layers experiment, *J. Geophys. Res.*, *100*, 6605–6620, 1995.
- Shaw, W. J., J. H. Trowbridge, and A. J. Williams III, Budgets of turbulent kinetic energy and scalar variance in the continental shelf bottom boundary layer, *J. Geophys. Res.*, *106*, 9551–9564, 2001.
- Smith, P. C., R. W. Houghton, R. G. Fairbanks, and D. G. Mountain, Interannual variability of boundary fluxes and water mass properties in the Gulf of Maine and on Georges Bank: 1993–1997, *Deep Sea Res., Part II*, *48*, 37–70, 2001.
- Wright, W. R., The limits of shelf water south of Cape Cod, 1941 to 1972, *J. Mar. Res.*, *34*, 1–14, 1976.
- Wright, W. R., and C. E. Parker, A volumetric temperature/salinity census for the Middle Atlantic Bight, *Limnol. Oceanogr.*, *21*, 563–571, 1976.
- 
- S. P. Anderson, S. J. Lentz, A. J. Plueddemann, and R. K. Shearman, Department of Physical Oceanography, Woods Hole Oceanographic Institution, 266 Woods Hole Road, Woods Hole, MA 02543-1541, USA. (steve@horizonmarine.com; slentz@whoi.edu; aplueddemann@whoi.edu; rshearman@whoi.edu)
- J. Edson, Department of Applied Ocean Physics and Engineering, Woods Hole Oceanographic Institution, 266 Woods Hole Road, Woods Hole, MA 02543-1541, USA. (jedson@whoi.edu)